Supplementary Information:

S1: Supplementary Methods

Singular value decomposition (SVD) of native state unfolding.

To analyse the unfolding of the native state from single-molecule double-jump experiments performed on I27-I27 (as detailed in **Methods**), singular value decomposition (SVD) was employed due to the overlap of the native and denatured populations.

A moving-window analysis (see **Methods**) was applied to the transfer efficiency range -0.2 to 0.6 (20 bins). The resulting *E* histograms were combined into an $m \times n$ matrix, **A**, for m=20 bins and n time points. SVD analysis decomposes the matrix **A** into three matrices[38]: **U**, **S** and **V**:

$$\mathbf{A} = \mathbf{U}\,\mathbf{S}\,\mathbf{V}^{\mathbf{T}}$$

U is an $m \times m$ matrix whose columns form the "output" basis vectors (eigenvectors of $\mathbf{A}\mathbf{A}^{\mathrm{T}}$). **S** is an $m \times n$ diagonal matrix whose elements are the singular values, or weighting factors for every basis vector (the square roots of eigenvalues of $\mathrm{A}\mathrm{A}^{\mathrm{T}}$ and $\mathrm{A}^{\mathrm{T}}\mathrm{A}$). $\mathbf{V}^{\mathrm{T}}$ is a transposed $n \times n$ matrix whose columns form the "output" amplitude vectors (eigenvectors of $\mathbf{A}^{\mathrm{T}}\mathbf{A}$) that correspond to the kinetics of the process. The output of the SVD allows a reduced representation of the data matrix to be produced, which describes the data in terms of basis vectors and their associated time-dependent amplitude vectors, and the number of non-zero singular values required to reconstruct the data matrix are an estimate of the number of species involved in the reaction. The amplitude vectors containing significant kinetic information were fitted with a single exponential process giving the rate constants for the unfolding of the native state. See Fig. 3c and Supplementary Fig. 3.

S2: Supplementary Table

Supplementary Table 1: Relative populations of the misfolded state[a] for all tandem constructs refolded and 'never-unfolded' calculated as described in Methods.

		Percentage of Misfolded Species	
	Tandem	**Refolded**	**'Never-unfolded'**
Linker-free[b]	I27(C3)-I27(C83)	5.7±0.5	0.7±0.6
	I27(C3)-I32(C83)	4.6±0.6	0.8±0.3
	I27(C3)-I28(C83)[c]	0.6±0.1	0.5±0.2
Linker	I27(C3)-I27(C38)	5.5±0.2	0.7±0.1
	I27(C3)-I28(C83)[c,d]	0.4	0.4
	I27(C3)-I27-I27(C83):		
	Dimer-like misfolded state[e]	9±2	2.1±0.1[g]
	Monomer-like misfolded state[f]	2.8±0.6	0.6±0.3

[a] The misfolded state is defined as bursts with $E \geq 0.8$ or the integrated fit of the histogram peak for the high FRET population.

[b] In linker-free constructs there are no added residues between domains, while linker constructs have four added amino acids (RSEL) between domains.

[c] Only analysed by summing bursts assigned to each 'population' (as described in Methods)

[d] Values quoted for one measurement made for each experiment.

[e] Misfolded state where the dyes have the transfer efficiency of the natively folded two-domain tandem.

[f] Misfolded state where the dyes have the transfer efficiency of the natively folded monomer.

[g] Due to the overlap between the *E* ranges of the correctly folded and dimer-like misfolded state in the refolded tandem histogram, this value was estimated by quantifying the number of bursts within the *E* range corresponding to the dimer-like species that fall outside the fit of the correctly folded peak in the never-unfolded tandem histogram.

All errors quoted are the unbiased sample standard deviation calculated from two 8-10 hr measurements.

S3: Supplementary Figures

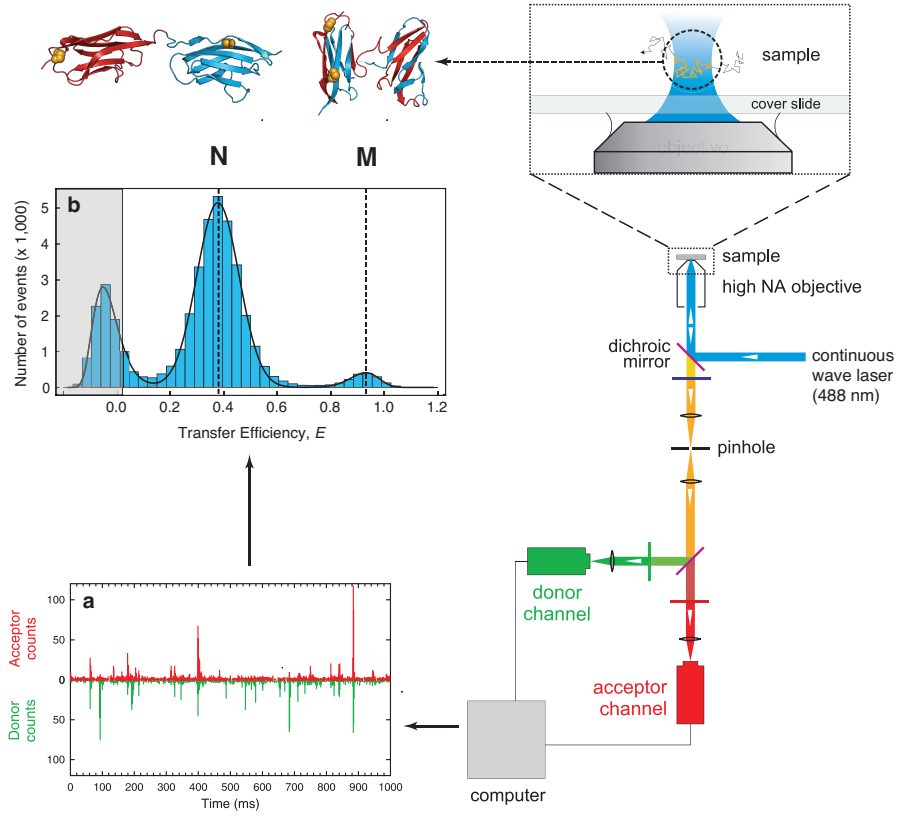

Supplementary Figure 1: Overview of a Single-Molecule FRET Experiment. The diagram on the right shows the main components of the instrument used. For these experiments, the proteins are labelled in specific positions with a suitable donor and acceptor fluorophore. If a protein molecule diffuses through the focused laser beam (circled; upper right), excitation of the donor may result in emission of a fluorescence photon or the transfer of the excitation energy to the acceptor, which can then emit a photon. (a) A typical signal trace of fluorescence photons detected in the donor and acceptor channels; each burst corresponds to a freely diffusing molecule passing thorough the confocal volume. The efficiency of the energy transfer, E, depends on the separation R of donor and acceptor via $E(R) = (1+(R/R_0)^6)^{-1}$, where R_0 is the Förster radius characteristic of the dye pair[4,10]. FRET can thus be used to map intramolecular distances in the range of 3 to 8 nm for the R_0 of 5.4 nm[39] used in this work. Experimentally, E can be calculated for each burst via $E = (n_A/n_A+n_D)$ where n_A and n_D are the corrected number of acceptor and donor photons detected, respectively (see **Methods**). (b) A two-dimensional histogram of a refolded sample of I27-I27, which shows subpopulations that can be attributed to the correctly folded (N) and misfolded (M) states, and molecules without an active acceptor[28] (shaded area).

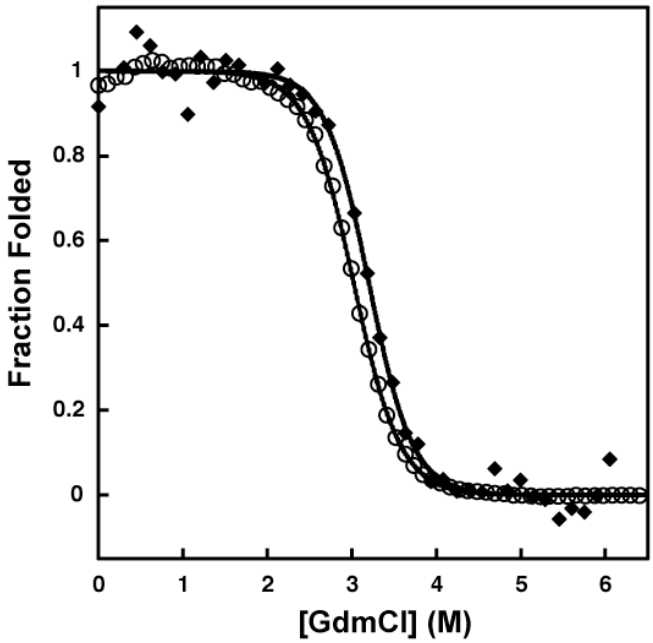

Supplementary Figure 2: Comparison of Ensemble Equilibrium Denaturation for I27wt and Doubly-Labelled I27. Fraction of protein folded as a function of denaturant concentration for I27wt (open circles) (data from reference 12) and doubly-labelled I27 (◆) with $\Delta G^{H_2O}_{D-N}$ of 7.6±0.1 and 8.0±0.1 kcal mol^{-1}, respectively (calculated using the average *m*-value, <*m*>,[12]). Mutation and labelling do not significantly alter the stability of I27.

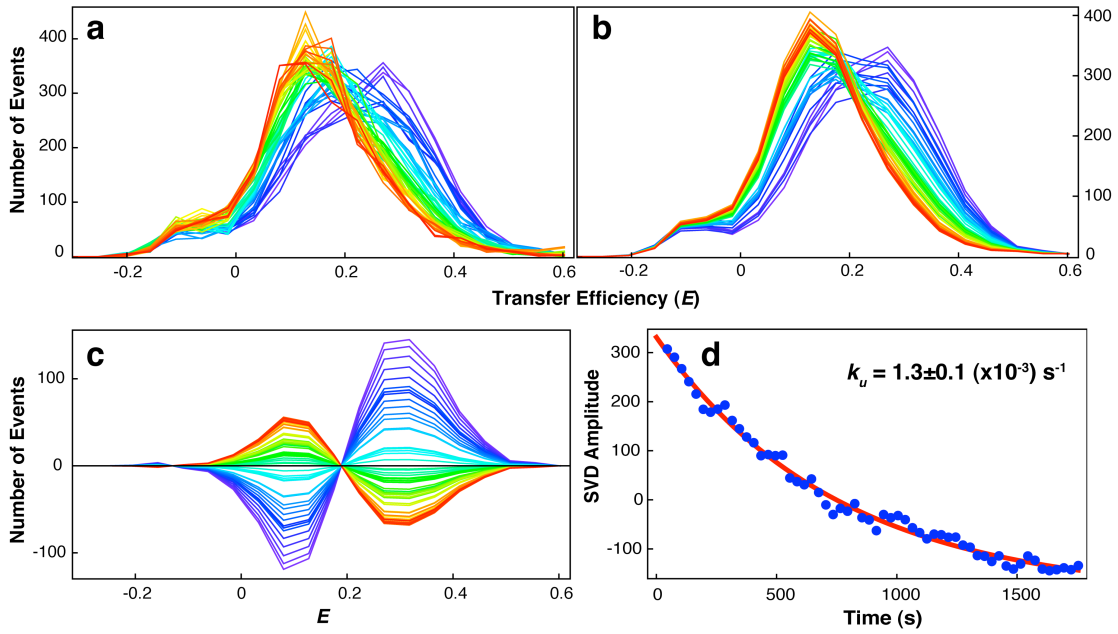

Supplementary Figure 3. SVD analysis of the Native State Unfolding in Single-Molecule Measurements. (**a**) Transfer efficiency histograms as a function of time (progressing from blue to red) of refolded doubly-labelled I27-I27 unfolding in 3.95 M (as described in **Methods**), for bursts where $-0.2 \leq E \leq 0.6$ (constructed as described in Supplementary Information). (**b**) Reconstructed transfer efficiency histograms from an SVD of the data in (**a**) using two components (which describes the process within experimental error). (**c**) Time evolution of the second basis vector from the SVD of the data in (**a**) (progressing from blue to red). (**d**) Kinetics from the second amplitude vector of the SVD of the data in (**a**) fitted to a single exponential process. It is noted that the first amplitude vector did not contain any kinetic information.

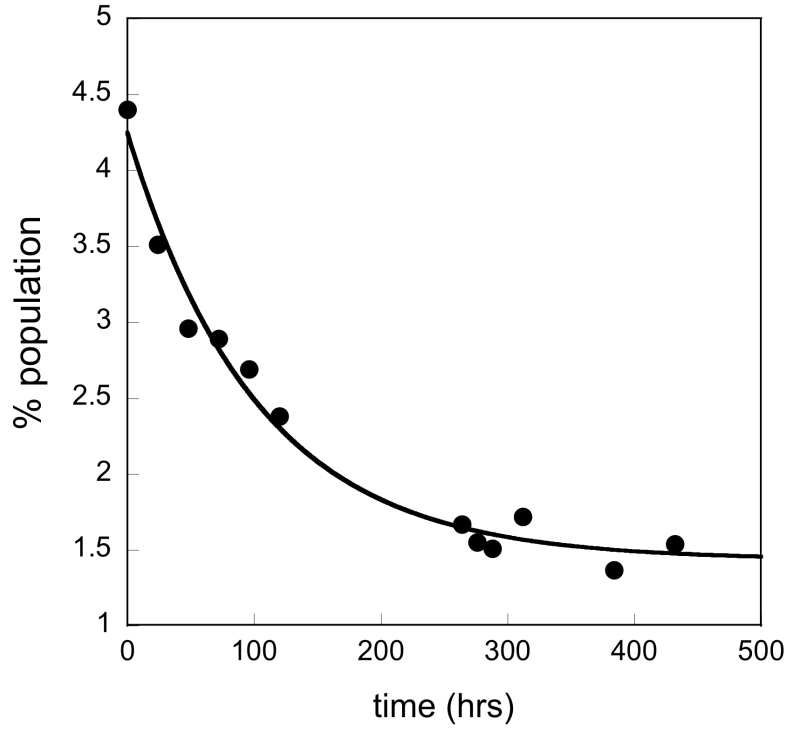

Supplementary Figure 4: Depletion of the Misfolded Species of I27-I27 Over Time in Absence of Denaturant. The points represent the fractional population of the misfolded species. Data are fitted with a single exponential function yielding a rate constant of 2.7×10^{-6} s^{-1}.

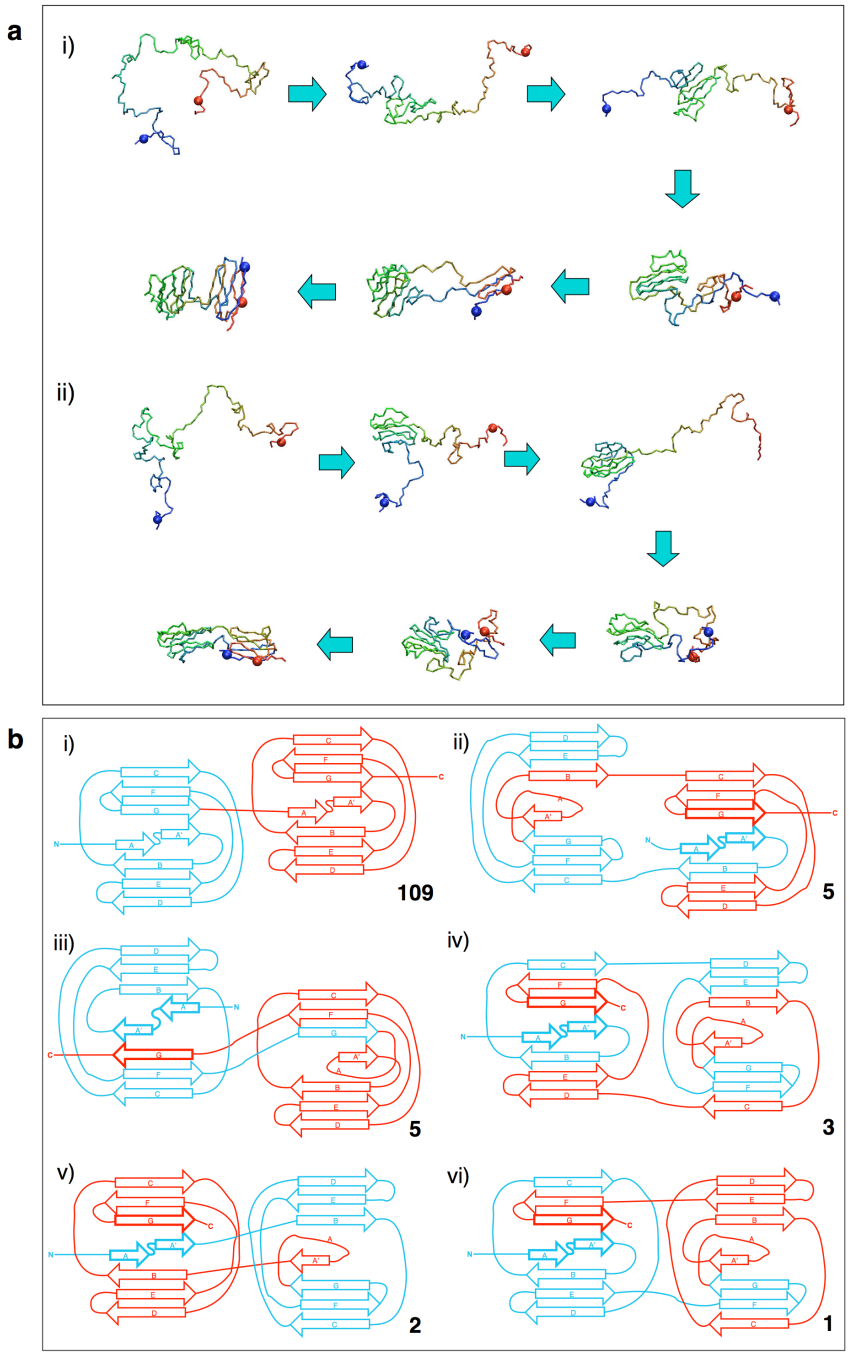

Supplementary Figure 5: I27-I27 Gō-like Model Folding Simulations: Trajectories and Topologies. (**a**) Two observed folding trajectories resulting in misfolded, strand-swapped topologies (i) and (ii) correspond to the topologies (vi) and (iv) in panel (**b**), respectively.) Attachment sites of the dyes are indicated by spheres (C3 in domain 1 and C83 in domain 2, blue and red, respectively). In all the misfolded topologies the central misfolded domain forms first. (**b**) All topologies seen in 125 completed trajectories. The number of trajectories which resulted in each topology annotated in bold: (i) the correctly folded, native tandem, (ii)-(vi) five strand-swapped topologies observed, classified as misfolded topologies. The N- and C- terminal strands, where the dyes are located, are shown in bold in the misfolded topologies.

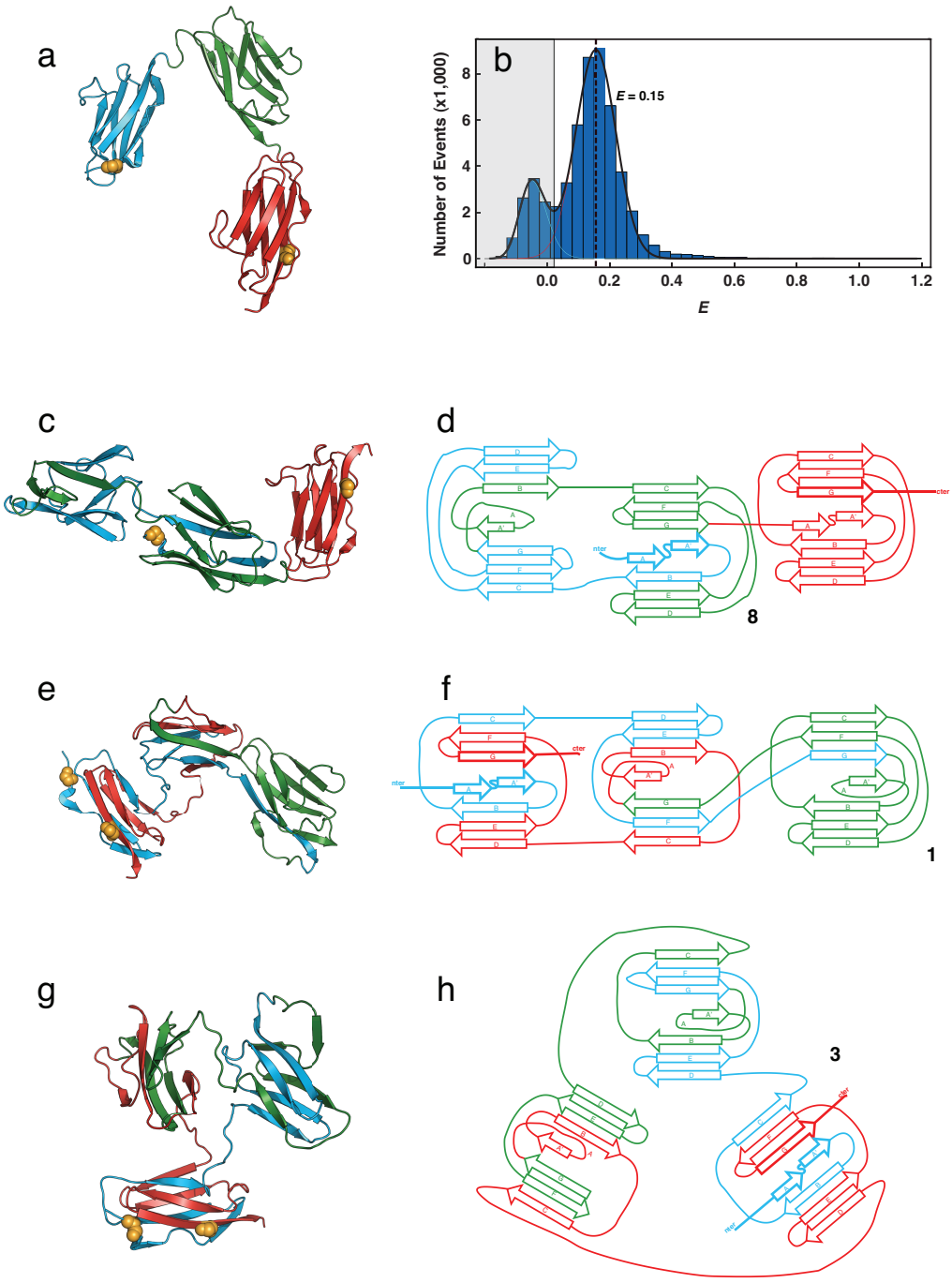

Supplementary Figure 6: I27-I27-I27 Gō-like Model Folding Simulations: Structures, Histogram and Topologies. (**a**) Natively folded I27-I27-I27 and (**b**) its "never-unfolded" histogram. 64 folding trajectories were generated: the numbers in black denote the number of trajectories which resulted in each topology shown. In total 18 trajectories resulted in "dimer-like" misfolded structures: the structure (**c**) and topology (**d**) are shown for one species formed, but all topologies are like those formed for I27-I27 (Supplementary Fig. 4) with a third domain correctly folded. 4 trajectories resulted in "monomer-like" misfolded structures, both of which are shown: structures (**e** & **g**) and topologies (**f** & **h**). In all structures the dye attachment sites are shown with golden spheres. In the misfolded topology diagrams the N- and C-terminal strands, where the dyes are located, are shown in bold.

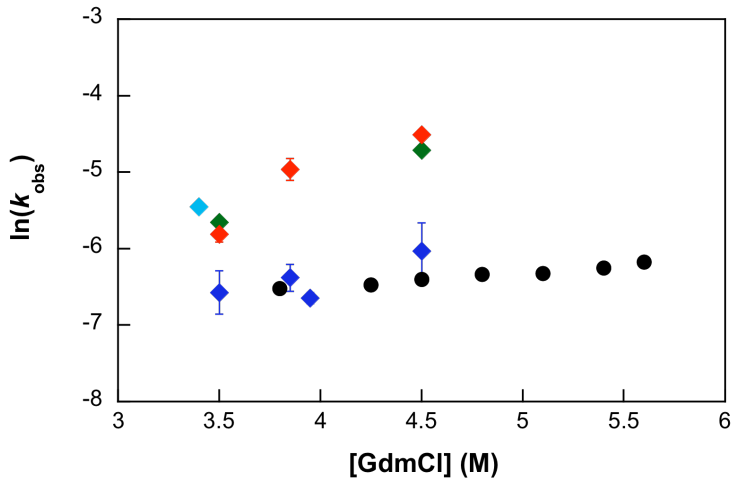

Supplementary Figure 7: Unfolding Rate Constants: I27wt from ensemble measurements (black circles[12]); native state of I27-I27 (with an RSEL linker) measured in single-molecule experiments (blue diamonds); misfolded states (all measured in single-molecule experiments) of I27-I32 (linker-free), I27-I27 (linker-free) and I27-I27 (with an RSEL linker), green, light blue and red diamonds, respectively. Note that error bars are plotted for all data points.

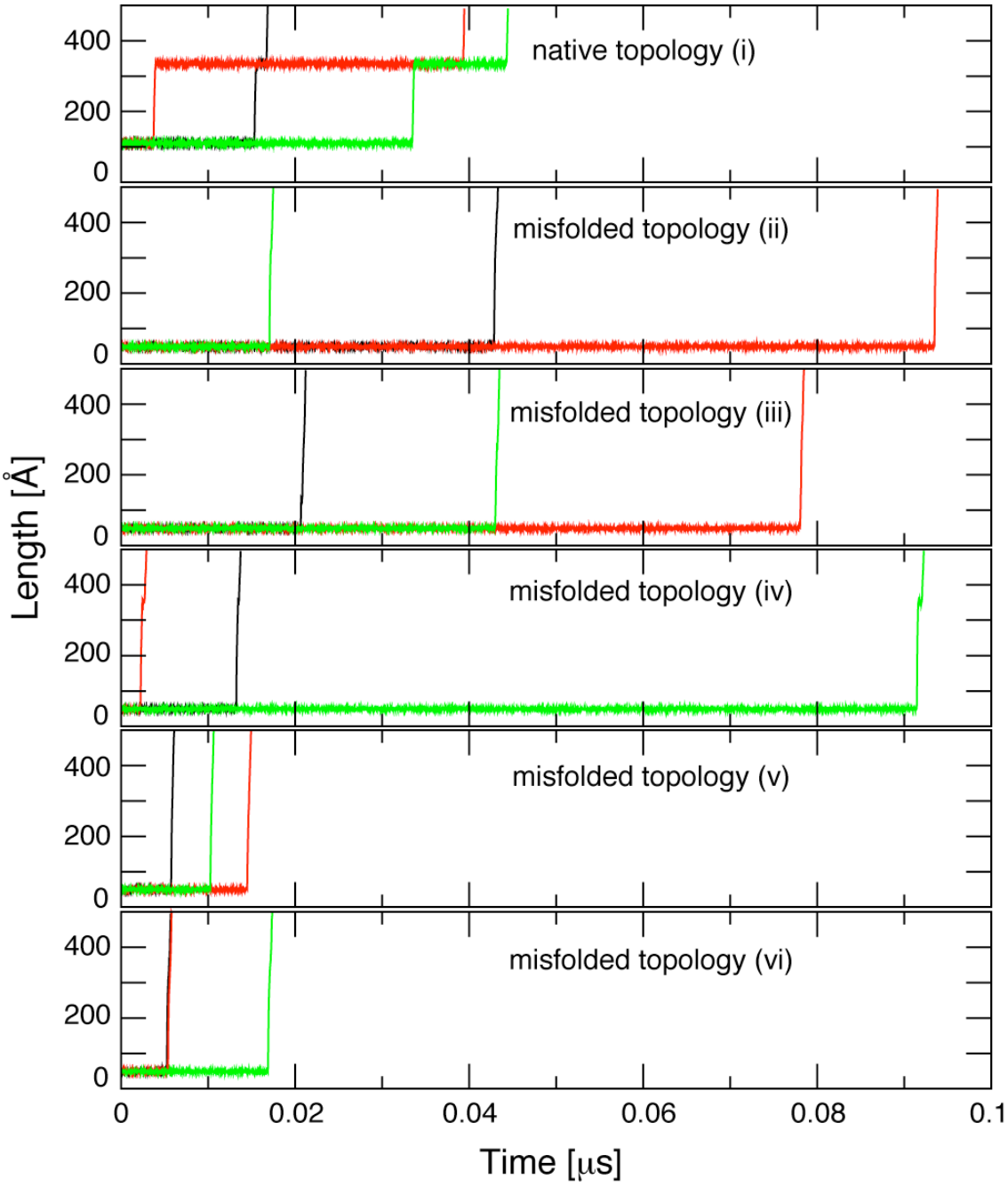

Supplementary Figure 8: Unfolding Trajectories in the Presence of a Pulling Force. Trajectories from simulations, run with a constant pulling force of 150 pN acting between the ends of the chain, for randomly chosen structures for each of the six I27-I27 topologies generated in the Gō-like Model Folding Simulations (Supplementary Figure 5). Three unfolding trajectories, initiated with a different random seed (denoted by different colours), were generated for each topology, monitoring the distance between the chain termini (simulations were terminated once the length exceeded 500 Å). (i)-(vi) numbering is as in Supplementary Figure 5. Only the native topology (i) shows a stable intermediate corresponding to having one domain unfolded with the other remaining folded; all misfolded topologies essentially unfold in one step as observed for the misfolded species in the AFM experiments[9].

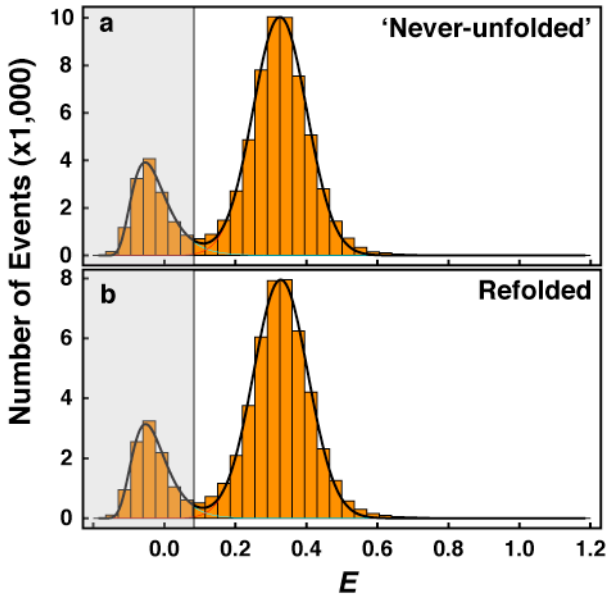

Supplementary Figure 9: Addition of a Linker does not Result in Misfolding in I27-I28. Transfer efficiency histograms for doubly-labelled I27-I28, with an RSEL linker between the domains, (**a**) 'never-unfolded' and (**b**) refolded. No misfolded species are formed. Histograms are fitted with Gaussian or log-normal distributions.

S4: Supplementary References:

38 Henry, E. R. & Hofrichter, J. Singular Value Decomposition - Application to Analysis of Experimental-Data. *Methods in Enzymology* 210, 129-192, (1992).

39 Schuler, B., Lipman, E. A. & Eaton, W. A. Probing the free-energy surface for protein folding with single-molecule fluorescence spectroscopy. *Nature* 419, 743-747, (2002).